Trajectory Models for Heavy Particles in Atmospheric Turbulence: Comparison with Observations

JOHN D. WILSON

Department of Earth and Atmospheric Sciences, University of Alberta, Edmonton, Alberta, Canada

(Manuscript received 2 July 1999, in final form 7 January 2000)

ABSTRACT

The simplest ''random flight'' models for the paths of heavy particles in turbulence have been tested against previous observations of the deposition of glass beads from an elevated source in the atmospheric surface layer. For the bead sizes examined (diameter 50–100 μm), for which the ratio of particle inertial timescale to turbulence timescale $\tau_p/\Gamma_L \ll 1$, it was found sufficient to adapt, as others earlier have done, a well-mixed first-order Lagrangian stochastic (''Langevin'') model of *fluid element* trajectories, simply by superposing a gravitational settling velocity w_g and reducing the velocity autocorrelation timescale along the heavy particle trajectory (Γ_p) relative to the fluid-Lagrangian timescale (Γ_L). That is to say, unless details of the particle distribution very close to ground (where τ_p/Γ_L is not small) are of interest, no advantage other than conceptual clarity can be found in the more faithful approach of explicitly modeling particle acceleration by means of the particle equation of motion.

With the timescale reduction parameter $\beta \sim 2$, the Langevin model estimated the location and width of the bead deposit swath very well and fixed the peak deposit density to within (at worst) about 100% error (in very stable stratification), but more generally to within about 20%. In the case where trajectories intersected a tall crop canopy, uncertainties in the treatment of deposition proved more significant than nuances of the trajectory algorithm.

1. Introduction

A better understanding of numerous technical and environmental processes hinges on our ability to calculate the paths $X_i = X_i(t)$ of heavy particles in turbulent flow. An example from engineering is control of the distribution of liquid fuel droplets in a combustion chamber, while in the atmospheric context, there is the challenge of better representing the distribution and deposition of aerial sprays, and the spread of plant pollen or disease spores.

Many approaches exist for the calculation of heavy particle trajectories. For complex, disturbed flows, a prerequisite task is calculation of the flow-field itself, perhaps by direct numerical simulation (Brooke et al. 1994; Pan and Banerjee 1996), or large-eddy simulation. Here, however, the discussion is limited to situations in which the flow itself is ''known,'' in the sense that its statistical structure is provided; and we focus on the most natural of particle dispersion theories, the ''random flight'' model, in which an ensemble of particle trajectories are computed in the given flow. Regarding alternative theories of heavy particle dispersion, much has been done to specify an effective (particle) eddy diffusivity (e.g., Yudine 1959; Csanady 1963; Reeks 1977;[1] and many others), but a general formulation, for arbitrary types of particles in inhomogeneous turbulence, is probably impossible (see section 2). Lightstone and Raithby (1998) proposed an empirical gradient-diffusion closure for the conservation equation governing the probability density function (pdf) for particle velocity, but its generality remains to be established. The appeal of the random flight method is its directness, due to which it is relatively free of theoretical obscurity.

Corresponding author address: John D. Wilson, Department of Earth and Atmospheric Sciences, University of Alberta, Edmonton, AB T6G 2E3, Canada.
E-mail: john.d.wilson@ualberta.ca

[1] Reeks gave an approximate solution for particle dispersion in stationary, homogeneous, isotropic Gaussian turbulence, inferring that ''in the absence of gravity, the asymptotic (i.e., large t) particle diffusion coefficient is in general greater than that for the fluid. Only when gravity and other external forces are imposed can this effect be reversed. . . .'' This finding illustrates the restricted validity of those formulas that do exist for particle eddy diffusivity.

Perhaps the most common heavy particle random flight model is the ''eddy interaction model'' (e.g., Graham 1996). This explicitly resolves particle acceleration d^2X_i/dt^2 [models of this character will here be called ''Inertial Particle'' (IP) models], but treats the ''driving'' fluid velocity $u_i[X_i(t)]$ at the location of the particle[2] as constant across ''patches'' of the fluid, and as changing discontinuously from eddy to eddy. Others attempt to more-realistically account for the time evolution of the driving fluid velocity (e.g., Sawford and Guest 1991). At a less faithful level of description, one may model the stochastic particle velocity U_{pi} itself directly, usually by means of a Langevin-type equation, which will require to be provided the heavy particle velocity variance, and the autocorrelation timescale (Γ_p) along the trajectory (e.g., Walklate 1987).

This paper investigates how well existing heavy particle trajectory models perform, relative to observations, in the best understood of turbulent atmospheric flows, the horizontally uniform atmospheric surface layer. Section 2 gives a brief overview of trajectory models, and in sections 3 and 4 several algorithms will be judged against field observations of the dispersion of glass beads, released from a tower at a height (h) a few meters above ground. It will be shown that the Langevin-type model suffices to obtain simulations that are about as accurate as we typically are accustomed to hope for in atmospheric modeling, and that the IP model offers no gain in accuracy.

2. Stochastic particle trajectory models

Taylor (1921) initiated the Lagrangian view of the turbulent dispersion of a passive tracer, which holds a fundamental advantage relative to Eulerian methods, namely, that there is no call for assumptions relative to *joint* moments of tracer concentration (c) and Eulerian velocity (u_i). The most common of such assumptions is the eddy diffusion model,

$$\overline{u_i' c'} = -K\frac{\partial \overline{c}}{\partial x_i}, \tag{1}$$

that is, the first-order closure for the tracer flux density, in terms of an eddy diffusivity (K). It is well known (e.g., Corrsin 1974; Wilson 1989) that K theory is inadequate wherever the scale of the turbulent eddies carrying the unresolved flux is not small relative to the scale of the dispersing plume or puff, for example, in the ''near field'' of a source, and higher-order Eulerian closures are compromised (Deardorff 1978) by assumptions with respect to higher-order joint statistics, for example, $\langle u_i' u_j' c' \rangle$.

a. A hierarchy of Lagrangian stochastic models for passive tracer dispersion

Wilson and Sawford (1996) reviewed the application of Lagrangian stochastic (LS) models for passive tracer dispersion in undisturbed atmospheric boundary layer flows. The ''zeroth-order'' LS model for motion along a single axis (say z, the vertical), is a random walk in position [the drunkard's walk, or Random Displacement Model (RDM)]. Over each time increment[3] dt the increment dZ in particle position is given by

$$dZ = a\,dt + b\,d\xi, \tag{2}$$

where a, b are deterministic coefficients, and $d\xi$ is drawn randomly from a Gaussian distribution with mean zero, and (by convention) variance dt. This model is easily shown to be equivalent to the treatment of turbulent convection as a diffusion process, and for stationary turbulence

$$a = \frac{\partial K}{\partial z}, \qquad b^2 = 2K. \tag{3}$$

The RDM is fundamentally wrong, and manifests as such close to a source. Although it may be adequate for description of the ''far field,'' there remains the objection that the eddy diffusivity is not strictly a flow property and is not directly measurable.

In the RDM, X_i is treated as Markovian, that is, correlation of particle velocity from one time step to the next is ignored; thus, the problem that the model is invalid for travel times short compared to the typical velocity correlation timescale. This deficiency is remedied in the ''first-order'' LS model, wherein the Markovian state variable is (X_i, U_i), and the velocity evolves in time according to a generalized Langevin equation (Thomson 1987),

$$dU_i = a_i\,dt + b_{ij}\,d\xi_j. \tag{4}$$

In order to uphold Kolmogorov's similarity theory $\langle dU_i dU_j \rangle = C_0 \varepsilon dt \delta_{ij}$ for the statistics of velocity increments over small dt, one specifies

$$b_{ij} = \sqrt{C_0 \varepsilon}\,\delta_{ij} \tag{5}$$

(ε is the rate of dissipation of turbulent kinetic energy, and C_0 is a dimensionless coefficient). Thomson provided a constraint on the other model coefficient, the vector a_i, to ensure that the LS model has the property that, should it hypothetically be applied to the motion

[2] The symbol X_i will denote position of a particle, or marked fluid element. Also, U_{pi} (or U_i) will denote the corresponding particle (or fluid-Lagrangian) velocity. Eulerian velocity will be designated u_i, mean values (e.g., of u_i) by $\overline{u}_i$ or by $\langle u_i \rangle$, and fluctuations relative to the mean by u_i', etc.

[3] The RDM supplies no criterion to limit the magnitude of the time step dt, other than inhomogeneity scales such as $K\,(\partial K/\partial z)^{-2}$. Choice of a time step is therefore arbitrary, whereas the Lagrangian autocorrelation timescale T_L naturally limits the time step of first-order models.

of tracer that is (already) well mixed in position-velocity space, the tracer would *remain* well mixed. In the case of an LS model for a *single* velocity component (say, W, the vertical velocity), the scalar coefficient "a" is uniquely determined by this "well-mixed condition," in terms of the probability density function $g_a(w)$ for the underlying Eulerian velocity field (w) of the flow. If we specify that g_a is Gaussian, a useable choice in treatment of the atmospheric surface layer, then the unique, well-mixed, first-order LS model for the (fluid element) vertical velocity is

$$dW = \left[-\frac{C_0\varepsilon(Z)}{2\sigma_w^2(Z)}W + \frac{1}{2}\frac{\partial\sigma_w^2}{\partial z}\left(\frac{W^2}{\sigma_w^2} + 1\right)\right]dt + \sqrt{C_0\varepsilon}\,d\xi$$
$$dZ = Wdt. \tag{6}$$

The factor $2\sigma_w^2(C_0\varepsilon)^{-1}$ can be interpreted as being effectively a Lagrangian correlation timescale T_L, in which case we may rewrite $b = (C_0\varepsilon)^{1/2}$ as $b = (2\sigma_w^2/T_L)^{1/2}$. The one-dimensional model [Eq. (6)] serves as the underlying velocity-evolution model for most of the heavy particle trajectory simulations reported here, using both the Langevin and the IP classes of model. It simplifies to the (basic) Langevin equation if the velocity variance σ_w^2 is homogeneous along the vertical. The influence of atmospheric stratification enters through the turbulence parameters and the mean velocity profile $\overline{u}(z)$.

The well-mixed constraint does not select a unique multidimensional LS model. Where simulations have included the Lagrangian alongwind velocity fluctuation U', Thomson's two-dimensional model for Gaussian inhomogeneous turbulence has been used, that is,

$$dU' = -\frac{b^2}{2\sigma^2}\left(U'\sigma_w^2 - W\overline{u'w'}\right)dt + \frac{\varphi_u}{g_a}dt + bd\xi_u$$
$$dW = -\frac{b^2}{2\sigma^2}\left(W\sigma_u^2 - U\overline{u'w'}\right)dt + \frac{\varphi_w}{g_a}dt + bd\xi_w$$
$$dX = [\overline{u}(Z) + U']dt$$
$$dZ = Wdt. \tag{7a}$$

Here, $g_a(U', W)$ is the height-dependent (Eulerian) joint velocity pdf; $\sigma^2 = \sigma_u^2\sigma_w^2 - u_*^4$; and the φ's are given by

$$\frac{\varphi_u}{g_a} = \frac{1}{2}\frac{\partial\overline{u'w'}}{\partial z} + \frac{1}{2\sigma^2}\left[\frac{\partial\sigma_u^2}{\partial z}\left(\sigma_w^2U'W - \overline{u'w'}W^2\right) + \frac{\partial\overline{u'w'}}{\partial z}\left(\sigma_u^2W^2 - \overline{u'w'}U'W\right)\right]$$

$$\frac{\varphi_w}{g_a} = \frac{1}{2}\frac{\partial\sigma_w^2}{\partial z} + \frac{1}{2\sigma^2}\left[\frac{\partial\sigma_w^2}{\partial z}\left(\sigma_u^2W^2 - \overline{u'w'}U'W\right) + \frac{\partial\overline{u'w'}}{\partial z}\left(\sigma_w^2U'W - \overline{u'w'}W^2\right)\right]. \tag{7b}$$

Note that the fluctuations U' and W have been simulated using the same timescale (Γ_L) and model coefficient $b = (2\sigma_w^2/T_L)^{1/2}$. Equations (7) simplify considerably in the case of a constant stress layer (e.g., as in simulations of section 3).

A first-order LS model, like Eqs. (6) or (7), correctly predicts the rate of dispersion even in the near field of a source, where travel time t is *not* large w.r.t. Γ_L, in contradistinction to the RDM and to Eulerian models. Of course, the trajectories are *not* valid for travel times on the order of the *acceleration* timescale. To treat such exceptionally short-range trajectories, or trajectories in low Reynolds number turbulence, one may introduce a second-order LS model (e.g., Du et al. 1995). In this case the Markovian state variable is (X_i, U_i, A_i), where A_i is the acceleration, modeled as $dA_i = a_idt + b_{ij}d\xi_j$.

b. Inertial-particle trajectory models

The weaknesses of the Eulerian approach, and in particular of K-theory closure, carry over to the case of dispersing particles. The restricted validity of existing formulas for particle eddy diffusivity has already been mentioned, and the trajectory-simulation approach seems the best way to circumvent the difficulty. But how ought the particle trajectories to be constructed?

Let us assume rigid, nonrotating spherical particles, whose density ρ_p greatly exceeds the fluid density ρ. Then a simplified particle equation of motion can be adopted, and for the purposes of this paper it will suffice that we define the IP class of particle trajectory models to have the form

$$\frac{dU_{pi}}{dt} = \frac{u_i(X_i) - U_{pi}}{F(t)} - g_i$$
$$du_i = a_i[X_i, u_i, (u_i - U_{pi}), \ldots]dt + b_{ij}d\xi_j$$
$$dX_i = U_{pi}dt. \tag{8}$$

If we assume further that the slip Reynolds number $R_e = d|\mathbf{u}(\mathbf{X}) - \mathbf{U}_p|/\nu$ is small (d is particle diameter, and ν is fluid kinematic viscosity), then F = constant = τ_p, the particle acceleration timescale.

No obvious generalization of Thomson's well-mixed condition can be invoked to select the model coefficient a_i. For suppose at $t = 0$ we released into stationary, horizontally uniform turbulence, bounded on the inhomogeneous axis (z) by perfectly reflecting boundaries, a single particle. Suppose that this particle has mass (inertia), but that no body force affects it ($g_i = 0$). For sufficiently large t, whatever the initial position (fixed or random) of the particle, the system will move to an equilibrium, in the

sense that the (mean) vertical mass flux density will vanish, and statistics of the system will have attained constancy in time. What is the equilibrium particle distribution (on the z-axis) in such a system? Presumably the state of maximum entropy; but how is the entropy of this system defined? ''Turbophoresis'' must imply that the equilibrium particle distribution is nonuniform.

c. Turbophoresis

The existence of turbophoresis was first suggested[4] (and the effect named) by Caporaloni et al. (1975), who reasoned that a (mean) particle mass flux can occur in conjunction with a uniform particle distribution, in response to spatial inhomogeneity of the turbulent velocity fluctuations. By ''assuming that the motion of a particle under nonisotropic turbulent 'shocks' is analogous to the motion of a particle under asymmetrical molecular shocks (thermophoresis) as described by Einstein,'' they derived a formula for the turbophoretic drift velocity. Reeks (1983) gave a more formal analysis (an approximation for the evolution of the joint probability density function for particle position and velocity), deriving a turbophoretic velocity that is related to the spatial gradient in the *particle* mean-square velocity tensor (μ_{ij}),

$$U_{i,tf} = \tau_p \frac{\partial \mu_{ij}}{\partial x_j}. \quad (9)$$

Reeks cautioned, however, that ''the precise form of the turbophoretic term ... depends upon ... the closure approximation we adopt.'' It is interesting to note that turbophoretic drift occurs even in the case of particles in a flow that is inhomogeneous only by virtue of a gradient in turbulence timescale, such as the (idealized) neutrally stratified atmospheric surface layer, where, if we follow convention and overlook the ''Unresolved Basal Layer'' (Wilson and Flesch 1993) we have a system with constant velocity variance, but with timescale Γ_L decreasing to zero at the ground.

Reeks (1983) considers the turbophoretic term ''a manifestation of the skewness in the velocity distribution of the particle.'' In any case, as regards selection criteria for heavy-particle trajectory models, the well-mixed condition clearly does not apply in its original sense (even in the absence of body forces). A properly formulated heavy particle trajectory model should reproduce turbophoresis—but this will presumably arise quite naturally, for a large ratio τ_p/Γ_L (e.g., near the ground) will result in a reduced mean-square particle velocity ... and turbophoresis.

d. Heuristic models of the driving fluid velocity for IP models

In one of the earliest heavy-particle trajectory models to be developed after the provision (Thomson 1987; Pope 1987) of selection criteria for LS models of passive tracer dispersion, Sawford and Guest (1991) ''attempted to combine the understanding of heavy particle effects gained from studies in idealized stationary homogeneous turbulence with a good model of passive scalar dispersion for more realistic flows.'' Treating particle motion in decaying homogeneous isotropic turbulence (an analogue for grid turbulence), Sawford and Guest commenced from the well-mixed LS model for *tracer* dispersion,

$$dU_i = -u_i\left(\frac{1}{\Gamma} + \frac{\sigma^2}{2}\frac{d\sigma^{-2}}{dt}\right)dt + \sqrt{C_0\varepsilon}\,d\xi_i, \quad (10)$$

where $\Gamma = 2\sigma^2(C_0\varepsilon)^{-1}$ and σ^2 is the Eulerian velocity variance. Sawford and Guest reasoned that correlation in fluid velocity along a *heavy* particle trajectory should be reduced relative to correlation along a fluid element trajectory, so, the above (generalized) Langevin equation *with a reduced timescale* was considered to generate an appropriate driving fluid velocity for imposition in the particle equation of motion (their rationale for the timescale reduction is given in appendix A). Simulations were in quite good agreement with the laboratory (grid turbulence) experiments of Snyder and Lumley (1971).

Other IP models that perform comparably well relative to the limited observations available have been reported (e.g., Zhuang et al. 1989, whose IP model was more complex, in that the trajectories of both the heavy particle and a driving fluid element were tracked). IP simulations of section 4 evolve the driving fluid element velocity using the well-mixed fluid element trajectory model for Gaussian inhomogeneous turbulence [Eqs. (6) or (7)], the timescale (where noted) being reduced in the same manner as by Sawford and Guest.

e. Langevin class of particle trajectory models

Several authors [perhaps first Yudine (1959, and earlier), Csanady (1963), and others since] have suggested that for typical atmospheric problems, particle inertia is not very important, even, for example, for liquid droplets of diameter as large as $d = 400$ μm. Wilson et al. (1981) simulated their field experiments (glass beads, $\tau_p = 0.012$ s) by tacking a gravitational settling velocity ($w_g = 0.12$ m s^{-1}) to a first-order Lagrangian stochastic model for tracer trajectories. Recent treatments of aerial spray dispersion have taken the same line, and the main distinction between them rests on whether the underlying (tracer) trajectory model respects (or otherwise)

[4] Observation of turbophoresis is complicated. One seeks to observe a mean particle flux in the *absence* of a corresponding mean particle-concentration gradient, but, in natural systems a concentration gradient near boundaries generally occurs, due to particle deposition. Clear indication of the real existence of turbophoresis has been drawn from idealized direct numerical simulations (Brooke et al. 1994).

Thomson's well-mixed constraint (wmc); results of MacInnes and Bracco (1992), who examined several models *not* satisfying the wmc, usefully illustrate the seriousness of errors that can result. To give a few examples of these recent Langevin treatments of spray dispersion, Wang et al. (1995) adopted Thomson's two-dimensional well-mixed tracer dispersion model for a Gaussian velocity pdf [Eqs. (7)], and used Eq. (A1) to specify the correlation timescale Γ_p in terms of $T_L = 2\sigma_w^2(C_0\varepsilon)^{-1}$. Hashem and Parkin (1991) earlier had used a tracer model predating the well-mixed constraint, and reduced Γ_p relative to T_L according to an equation differing from (A1). Wallace et al. (1995) also used an old LS tracer model (though it may have been well mixed), but did not reduce Γ_p.

In none of these Langevin treatments of aerial spray was the particle vertical velocity variance (σ_{wp}^2) treated as distinct from (i.e., potentially smaller than) the fluid Eulerian velocity variance σ_w^2. On that point, while the ratio σ_{wp}/σ_w is known for some idealized cases, such as ''oscillating Stokes flow'' (e.g., Wilson et al. 1988), in general its value is inaccessible, and any theory fixing it implicitly has already solved the heavy particle trajectory problem. In their Langevin model for transport of evaporating ocean sprays, a model based on the Legg and Raupach (1982) LS treatment for passive tracer, Edson and Fairall (1994) reduced both σ_{wp} and Γ_p relative to their counterparts for a fluid element trajectory, invoking to that end formulas drawn from analytical studies. Essentially the same treatment was adopted by Lakehal et al. (1995) in calculations of raindrop trajectories in complex, urban wind flows.

If a Langevin-type model is adopted, and it *is* a well-mixed model (according to Thomson's criterion), then it cannot reproduce turbophoresis; for even if provided the (proper) near-ground gradient in *particle* velocity variance, by virtue of being a well-mixed model it will present a well-mixed state as the equilibrium condition. This objection to the Langevin class of model does not appear to be very serious, for in problems of practical interest, only *very* close to ground is τ_p/Γ_L sufficiently small to induce turbophoresis.

f. Notation and numerical details, for models to be tested against observations

In section 3, the following trajectory models (and variations thereof) will be compared with observations:

- RDM: Eq. (2) with superimposed gravitational displacement $w_g\Delta t$ for each time step Δt; coefficients as in Eq. (3), with $K = \sigma_w^2 T_L$. Time step $\Delta t = T_L(h)$, or $\Delta t = 0.1T_L(h)$, or $\Delta t = 0.1T_L(z)$.
- Sticky Fluid Element Model (SFE): Langevin model [Eqs. (6)]. Heavy particles are treated as fluid elements (no inertia or gravitational settling), but on contact with ground are deposited. For all Langevin-type models, $dt = 0.1\Gamma_p$, and unless otherwise stated, $\sigma_{wp} = \sigma_w$.
- Settling Sticky Fluid Element Model (SSFE): Langevin model [Eqs. (6)], modified only in so far as a constant gravitational settling velocity is superposed on the vertical velocity, that is, $dZ = (W + w_g)dt$, and ground is treated as perfectly absorbing surface.
- Two-dimensional Settling Sticky Fluid Element Model (SSFE + U'): Two-dimensional Langevin model [Eqs. (7)], with superposed settling velocity.
- Settling Sticky Fluid Element, Reduced Γ (SSFET): Langevin model, with superposed settling, and with Γ_p reduced to account for eddy fallout (crossing trajectory) effect.
- Inertial Particle: Driving fluid velocity calculated with Γ_p reduced to account for eddy fallout; $dt = 0.1\ \min(\tau_p, \Gamma_p)$.

3. Simulations of Suffield heavy particle dispersion trials

Hage (1961) and Walker (1965) reported observations of the deposition of glass beads (mass mean diameter d = 49, 56, or 107 μm), released continuously over durations of 30–60 min, from a point source at height h = 7.4 or 15 m over prairie land at the Suffield Research station in southern Alberta, Canada. Fifteen such trials covered a wide range in atmospheric stratification, and for each trial micrometeorological data are available, including the mean wind speed $\overline{u}(z)$ at heights z = 0.5, 1, 2, 4, 8, and 16 m, and the mean temperature difference between z = 0.5 m and z = 4 m. Appendix B documents how the surface layer scales u_*, L, z_0 have here been determined for each trial (see Table 1), as well as the velocity statistics that have been assumed for simulations. Appendix C describes how the reported particle size distribution was represented.

a. Regularity and credibility of the observed deposition pattern

The number-density of beads deposited [n, (m^{-2})] was observed as a function of azimuth θ and downwind distance x, on arcs at increasing radii up to (in some trials) a maximum x of 1100 m. By attributing to each particle an identical mass M (kg), Hage and Walker constructed from $n(x,\theta)$ a normalized, crosswind-integrated mass density

$$D_0(x) = \frac{M}{Q}\int n(x,\theta)x\, d\theta, \tag{11}$$

where Q (kg s^{-1}) is the source strength. Hage reported that graphical integrations for the ''recovery'' $R_o = \int_0^X D_0(x)\, dx$ indicated that the fraction of released mass deposited in the array ranged from 0.85 to 1.05 (trials 1–9), while Walker cited recoveries ranging from 0.65 to 1.00 (trials A–L). Observed deposition $D_0(x)$ is subject to some small degree of error due to the assignment

TABLE 1. Surface-layer scaling parameters for the glass bead dispersion trials at Suffield, Alberta [derived from information provided by Hage (1961) and Walker (1965)].

Walker's label	Hage's label	h (m)	d (μm)	u^* (m s^{-1})	L (m)	$z0$ (m)	wg/u^*	Recovery
A	2	15	107	0.35	30	0.037	1.66	1
B	3	15	107	0.39	104	0.014	1.49	1.11
C	5	15	107	0.44	341	0.025	1.32	0.89
D	6	15	107	0.39	107	0.028	1.49	0.94
E	8	15	107	0.59	−86	0.014	0.98	1.05
F	9	15	107	0.42	−41	0.031	1.38	0.98
G		7.42	56	0.21	52	0.043	0.9	0.92
H		7.42	56	0.28	35	0.004	0.68	0.91
I		7.42	56	0.18	16	0.016	1.06	1.17
J		7.42	49	0.51	−105	0.021	0.27	0.71
K		7.42	49	0.47	−48	0.017	0.3	0.82
L		7.42	56	0.57	−50	0.012	0.25	0.74

of equal masses to all observed particles, and unless the streamwise integration for R_o extends adequately far downwind, there is no requirement that $R_o = 1$. But the form of the $D_0(x)$ profiles given strongly suggests the observational array provided sufficient downwind span, and so one suspects serious experimental error (perhaps a subperiod of lateral drift carrying particles outside the array of deposition cards) in any trial for which $|R_o - 1|$ exceeds about 0.1 and certainly 0.2.

For each trial, observed recovery R_o was here estimated (see Table 1) by integrating $D_0(x)$, using piecewise linear interpolation between observations. Values of R_o so-calculated ranged from 0.71 to 1.17, a rather different outcome than was cited by Walker (0.65–1.00). The discrepancy may be due to use of different interpolations for the integration. For trials J, L the present estimate of $|R_o - 1|$ is almost 0.3, while for all other trials $|R_o - 1| \leq 0.2$, and in particular for trials A–H, $|R_o - 1| \leq 0.11$. On these grounds (fraction of released mass accounted for) one may place reasonable confidence in trials A–H.

Figures 1a,b show the horizontal profile of the crosswind-integrated deposition rate D_0, for six trials having $d = 107$ μm ($w_g = 0.6$ m s^{-1}, $\tau_p = 0.06$ s) and $h = 15$ m. Trial A ($R_{oA} = 1.00$) during most strongly stable stratification exhibits the narrowest deposition swath, with latest onset (plume arrival at ground delayed), and (at center) the highest deposit density. Conversely trial F ($R_{oF} = 0.98$) representing most strongly unstable stratification shows earliest onset, wider (but not *widest*) spread, and lower peak density. There the regularities stop: trials B, D ($R_{oB} = 1.11$, $R_{oD} = 0.94$) ought to show identical $D_0(x)$, on the basis of their nearly identical surface-layer state (u_*, L); one might hope to blame this irregularity on variability of the ratios $\sigma_{u,v}/u_*$ due to varying large-eddy energy (a variability not accounted for by u_*, L); but that hope is ill-founded for, as will be shown, simulations are rather indifferent to the inclusion of the fluctuation U'. On the basis of observed R_o, presumably trial D ought to be preferred over trial B (and happily, simulations to be reported agree better with trial D than with B). Not much improvement is gained as regards the ordering of the peak deposit densities, when D_0 is multiplied by a reference wind speed to provide a deposit-density profile D_0U_{15} normalized against varying wind speed (and implied plume dilution). However, one gains a perfect ordering of the swath leading edge (Fig. 1b).

Figure 2 gives the deposit pattern for trials with smaller beads ($d = 49$, 56 μm; $w_g = 0.14$, 0.19 m s^{-1}) released from a lower source at $h = 7.42$ m, in comparison with the (h, d, w_g) = (15 m, 107 μm, 0.58 m s^{-1}) observations. Again for the lower source, the leading edge of the deposit swath is positioned farther upwind in unstable than in neutral or stable stratification, and peak deposit densities are highest in stable stratification, a feature which is (once again) not explainable in terms of plume dilution (peak values of D_0U_{15} are not invariant across trials). Stable (unstable) stratification leads to the narrowest (widest) swath from the lower source. Figure 2 shows that although the ''fall time'' h/w_g is actually larger for the trials with the lower source (39 or 53 s, versus 26 s for the higher source, this being due to the smaller beads used), the position of the core of the deposit swath is only marginally shifted, and at that, upwind.

Figures 1 and 2 span a narrow range of an experimental parameter space (u_*, L, d, h) that might potentially admit a rich range of $D_0(x)$ patterns. There is no basis to expect these data should be easily ''collapsed'' by normalization, and one need not be disconcerted that they manifestly do not. The lack of a simple and unambiguous visually discernable pattern does not imply a lessened value of these data as a criterion for particle dispersion models. In the comparisons to follow, trial F will be taken to represent strongly unstable stratification; trial C near-neutral stratification; and trial A strongly stable stratification.

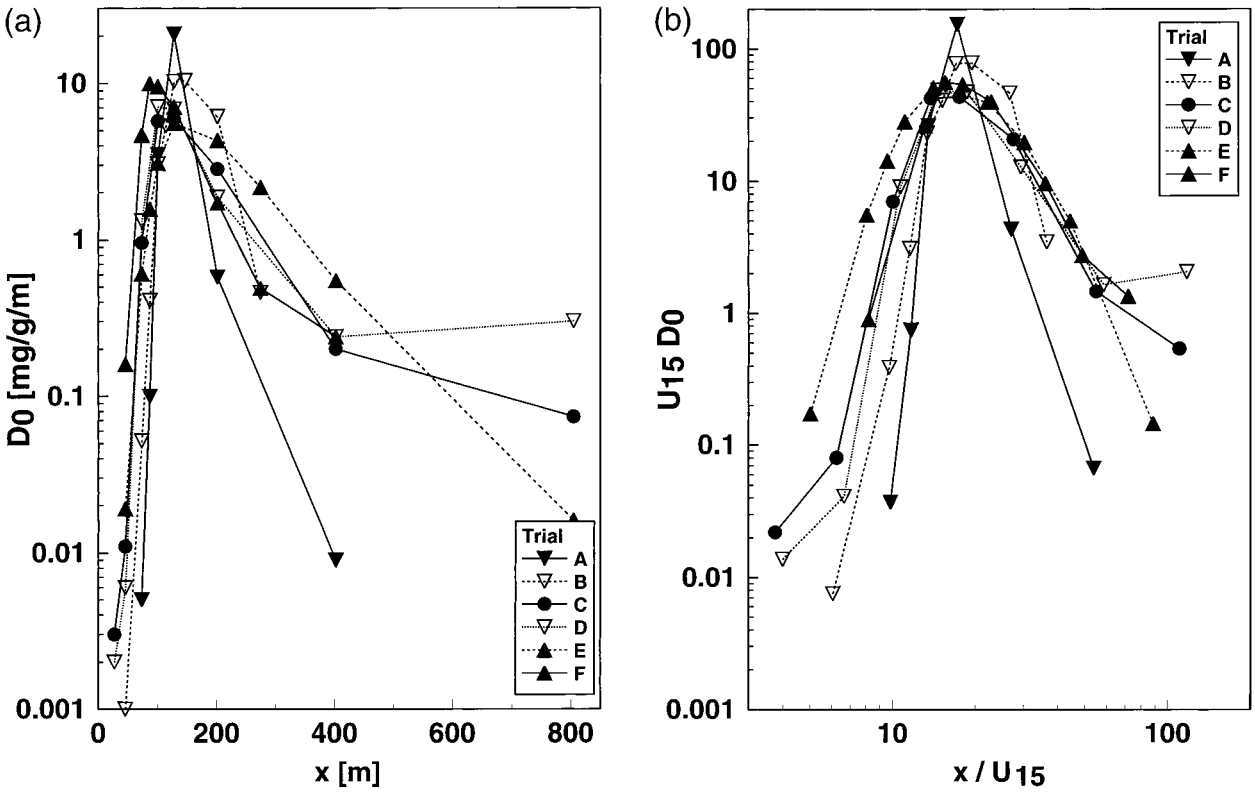

FIG. 1. (a) Observed crosswind-integrated deposition rate D_0 (mg g^{-1} m^{-1}) vs downwind distance x, for 107-μm glass spheres released continuously from a source at $h = 15$ m. Trials are labeled according to Walker (1965); D_0 is normalized on the source strength Q (g s^{-1}). Symbols suggest the effect of stratification on the plume spread (▲ = unstable; ● = near-neutral; ▼ = strongly stable). (b) Observations of (a) rescaled as $U_{15}D_0$ vs nominal travel time x/U_{15}.

b. Results of simulations

In simulations $N_p \geq 4 \times 10^5$ particles were released; ground deposition rate was resolved in collectors of width $\Delta x = 1$ or 4 m, the particles being deposited whenever they crossed the level $z = z_0$.

Figure 3a compares a sequence of the most rudimentary of Lagrangian models with the observations of the surface deposition pattern of the neutral Trial C ($R_{oC} = 0.89$). The ''no-turbulence impact point'' for this trial, that is, point of impact if a particle should simply fall at its terminal velocity [so that its height $Z(t) = (h - w_g t)$] while undergoing horizontal translation at a velocity $dX/dt = \overline{u}(Z(t))$, is $X_b = 159$ m. The peak in the observed deposit pattern occurs slightly upstream from X_b. Unsurprisingly, when the beads are treated as sticky fluid elements, the onset of the deposit swath is too far downstream, and the deposit swath is too wide, essentially a plateau stretching far downwind from X_b. The RDM (here implemented with timestep $\Delta t = \Gamma_L$), which accommodates particle settling and surface adhesion, positions the leading edge of a too-wide deposit swath too far upstream, underestimates peak density, and overestimates density far from the source.

At this point it is useful to consider the ''range'' of these Suffield diffusion trials. We may define a normalized travel time

$$\frac{x}{\overline{u}(h)T_L(h)} \approx \frac{k_v \dfrac{\sigma_w}{u_*} x}{\alpha h \ln\left(\dfrac{h}{z_0}\right)} \approx \frac{x}{h \ln\left(\dfrac{h}{z_0}\right)}, \qquad (12)$$

from the source to any downstream range (x), and taking $x \approx 100$ m, that is, the location of peak deposition for trial C, one finds $x/\overline{u}(h)\Gamma_L(h) \approx 1.0$. By this criterion, we should regard the Suffield trials as examining the ''near field'' of the source, within which a strong memory of the initial (release) velocity is sustained. Recall that in the (very) near field of a source in homogeneous turbulence, Taylor's (1921) theory gives for the rms displacement (i.e., plume spread) the result $\sigma_z = \sigma_w x/\overline{u}$, i.e., there is asymptotically (small travel time t or travel distance x) no sensitivity to the autocorrelation timescale. The RDM simply does not handle the near field, and its poor performance here is therefore unsurprising. Returning to Fig. 3a, rather good agreement with the observations results (SSFE), by using a Langevin class model as for a fluid element, but with an added settling

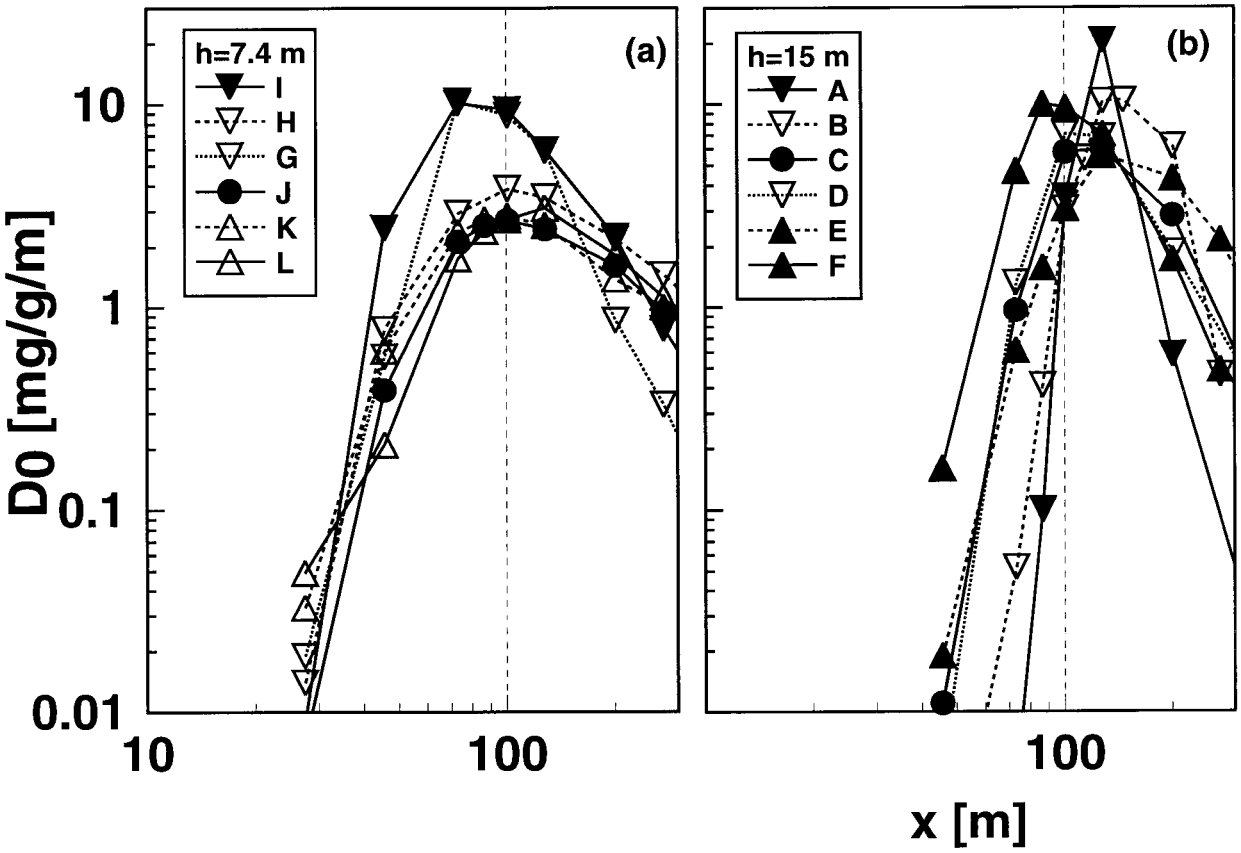

FIG. 2. Comparison of the observed deposit patterns for source heights $h = 7.4$, 15 m.

velocity w_g, and surface adhesion. To be sure this model (and the more complex simulations of Fig. 3b to follow) overpredicts D_0 far downstream at $x = 400$ m, but perhaps not much need be made of this in view of the remarkable fidelity overall.

Figure 3b displays the results of simulations with various refinements of the Langevin model, as well as with the more time-consuming IP model. Results from the IP model are identical to those from the corresponding Langevin model. This has always been found to be the case, or at least no convincing exceptions have been noted, provided equal values are assigned for β and other physical or numerical parameters; and it is no doubt to be expected, provided that over the greatest part of the trajectories, $\tau_p \ll \Gamma_p$. However, an IP model is in principle needed, if one wished to resolve details of the particle distribution very near the surface, where τ_p/Γ_p is not small.

Figure 3b shows that inclusion of the alongwind fluctuation U' is evidently of minor import in this case. The step of recognizing Γ_p as being smaller than Γ_L does improve model agreement with the $x = 400$ m observation and does a better job of positioning the upwind edge of the deposit swath. As far as this particular trial is concerned, the optimal value of β for the vertical velocity component, which would be 3/2 if one simply took over the findings of Sawford and Guest (see appendix A), is smaller than 2. But as the recovery for this trial $R_{oC} = 0.89$, an optimization is scarcely justifiable. As to the impact of reducing σ_{wp} relative to σ_w, which is arguably necessary near ground where τ_p/Γ_p in principle becomes large (particle inertia limiting particle response to rapid velocity fluctuations), the simplest such parameterization (e.g., Walklate 1987; Edson and Fairall 1994),

$$\frac{\sigma_{wp}^2}{\sigma_w^2} = \left(1 + c\frac{\tau_p}{T_p}\right)^{-1}, \tag{13}$$

had no observable impact on simulated $D_0(x)$; for example, for trial C, a simulation with $c = 1$ and $\beta = 2$ was indistinguishable from that (shown on Fig. 3b) with $c = 0$, $\beta = 2$.

Before closing the discussion of the quality of LS simulations of trial C, we return to the issue of this (and the other trials) being ''near field'' experiments, at least according to the observation that in the middle of the deposition swath $x/\overline{u}(h)\Gamma_L(h)$ is not large; then, could the demonstrated success of the higher-order models to some extent (even largely) rest on the fact of their up-

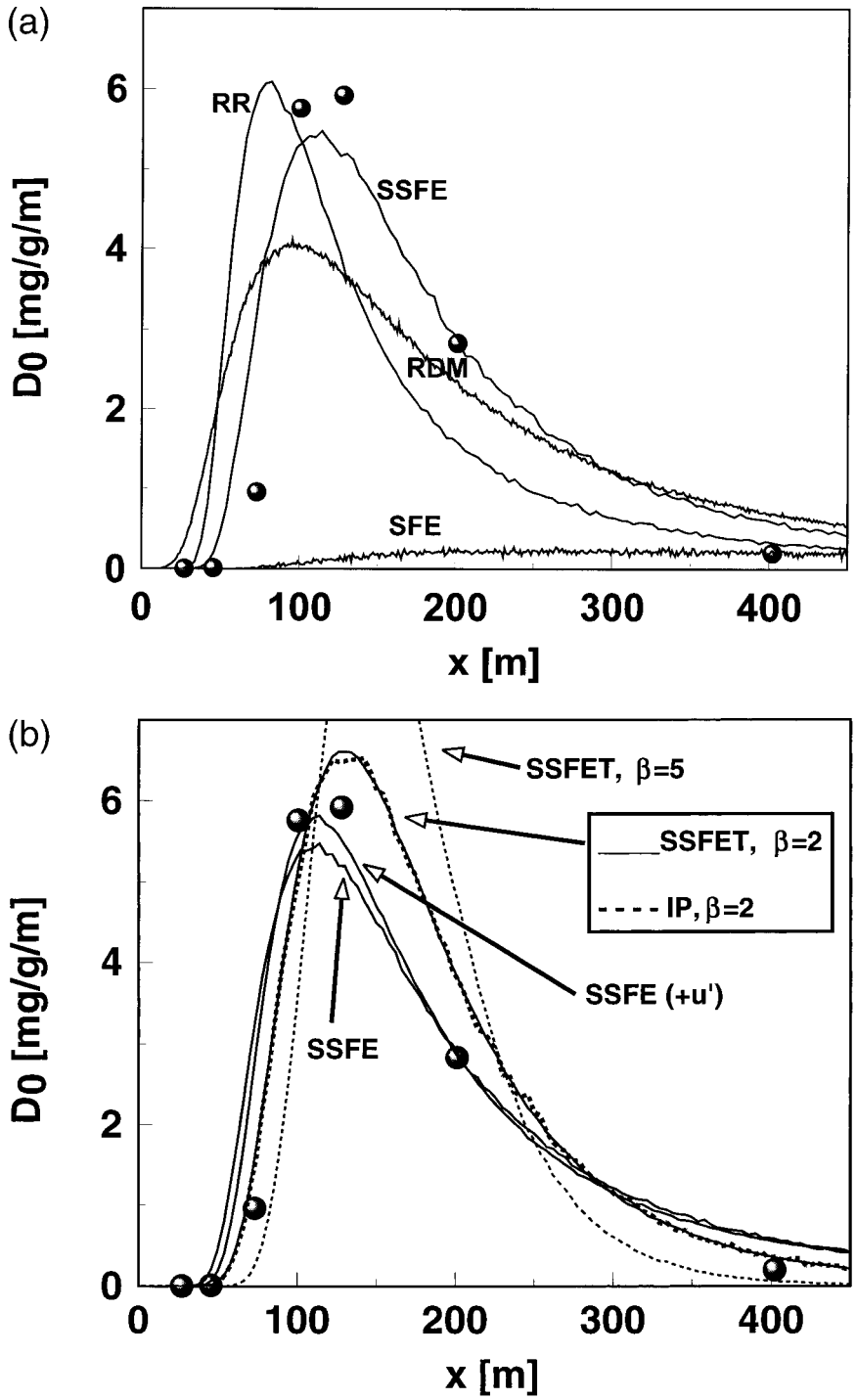

FIG. 3. Observations (●) and simulations of the along-wind profile of crosswind-integrated surface deposition rate, for the Suffield heavy particle dispersion trial C (near-neutral, $L = 341$ m; $R_{oC} = 0.89$). Particles ($w_g = 0.6$ m s^{-1}, $\tau_p = 0.06$ s) released at $h = 15$ m, and all models neglect u' unless noted. (a) Lagrangian stochastic simulations, in ascending order of complexity: RR, ''Random Release'' (release velocity sustained); RDM, ''Random Displacement Model''; SFE, ''Sticky Fluid Element''; SSFE, ''Settling Sticky Fluid Element'' (Langevin-class, with added w_g). (b) SSFE [as on (a)]; SSFE + u' (alongwind fluctuation included); SSFET, $\beta = 2, 5$ (Langevin model with w_g, and $\Gamma_p < T_L$); IP, Inertial Particle model with $\beta = 2$.

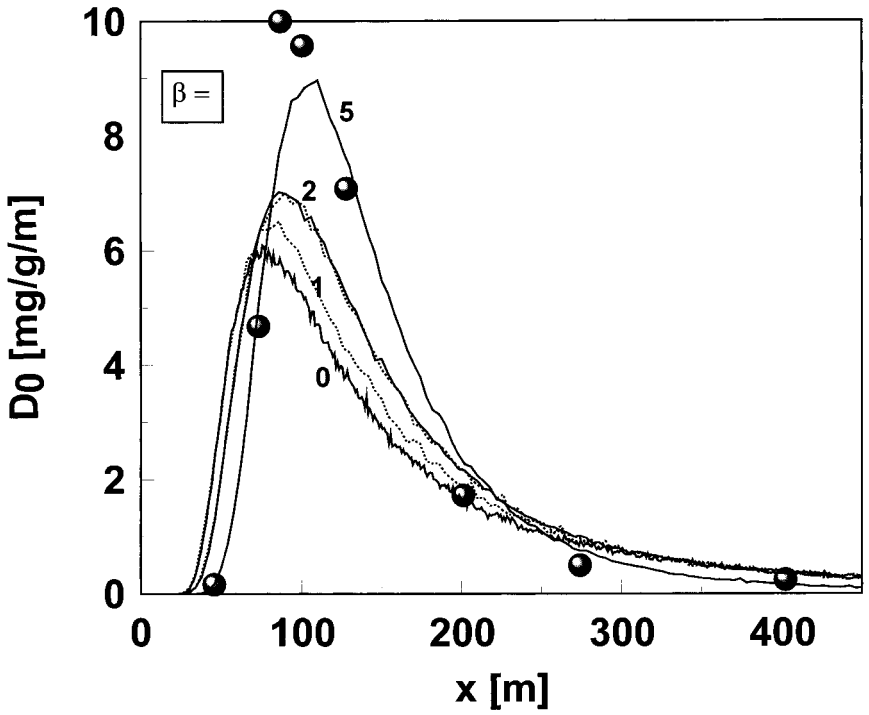

FIG. 4. Observations (●) and simulations of the along-wind profile of crosswind-integrated surface deposition rate, for the Suffield heavy particle dispersion trial F (unstable stratification, $L = -41$ m; recovery $R_{oF} = 0.98$). Particles ($w_g = 0.6$ m s^{-1}, $\tau_p = 0.06$ s) released at $h = 15$ m. Solid lines, Langevin simulations with $\beta = (0, 2, 5)$; dashed lines, Inertial Particle simulations with $\beta = (1, 2)$.

holding a realistic release velocity (randomly chosen from a Gaussian distribution whose variance σ_w^2 is securely known, through measured u_*) along a memory-dominated trajectory to ground? To test this possibility, trial C was simulated by releasing particles at the source ($z = h$) with the sum of the gravitational settling velocity and a random turbulent velocity from the Eulerian velocity probability density function, that is, $w = \sigma_w(h)\, r - w_g$, where r is a standardized Gaussian variate. This release velocity was sustained until particles were deposited or flew beyond the range of observations [the trajectory was resolved with time step $\Delta t = 0.001\Gamma_L(h)$]. The outcome, included on Fig. 3a as ''RR,'' is reassuring in that it confirms that the success of the random flight models *does* depend on their having a strong physical basis, and that the trajectories of these dispersion trials, while ''short,'' are not so short as to be insensitive to changes in the wind along their course.

Figure 4 compares observations and simulations of trial F ($R_{oF} = 0.98$), undertaken in strongly unstable stratification, for which the no turbulence impact point $X_b = 124$ m. For given β, the Langevin class and the Inertial Particle models yield identical results, while progressive reduction of the timescale ($\beta = 0, 1, 2, 5$) improves the positioning of the leading edge of the deposit swath, with correspondingly improved agreement over the entire range of x. A two-dimensional, Langevin simulation (SSFE + U' with $\beta = 0$), not shown, closely matches the results indicated on Fig. 4 for $\beta = 1$.

The observed deposit swath for trial A (stable stratification, $L = 30$ m; $R_{oA} = 1.00$) is narrow and strongly peaked. None of the simulations (Figs. 5a,b) match the observations very well at every x, but those with $\beta = 5$ are much better than with $\beta = 0$ or 2. The two-dimensional simulations of (5b) invoke the same fundamental timescale Γ_L for both velocity components; and where Γ_p is reduced relative to Γ_L, the fractional reduction is identical for U' and W. Addition of the alongwind fluctuation has insignificant impact; and neither does accounting for the size spectrum (see appendix C, and Table C1) achieve much gain.

Trials B and D (Fig. 6) ostensibly were undertaken in identical atmospheric conditions ($u_* = 0.39$ m s^{-1}; $L = +100$ m), but the outcomes $D_0(x)$ are distinct. Simulations show better agreement with trial D ($|R_{oD} - 1| = 0.06$) than with trial B ($|R_{oB} - 1| = 0.11$). As earlier noted, accounting for the particle size spectrum makes an insignificant difference to the model $D_0(x)$ except on the edges of the swath.

Figure 7 compares simulations with observations of the deposit pattern from a near-neutral trial ($L = -105$ m) with smaller (mass mean diameter $d_0 = 49$ μm) beads released at a lower level, $h = 7.42$ m (trial J, $R_{oJ} = 0.71$). The RDM gives poorest treatment. Simulations

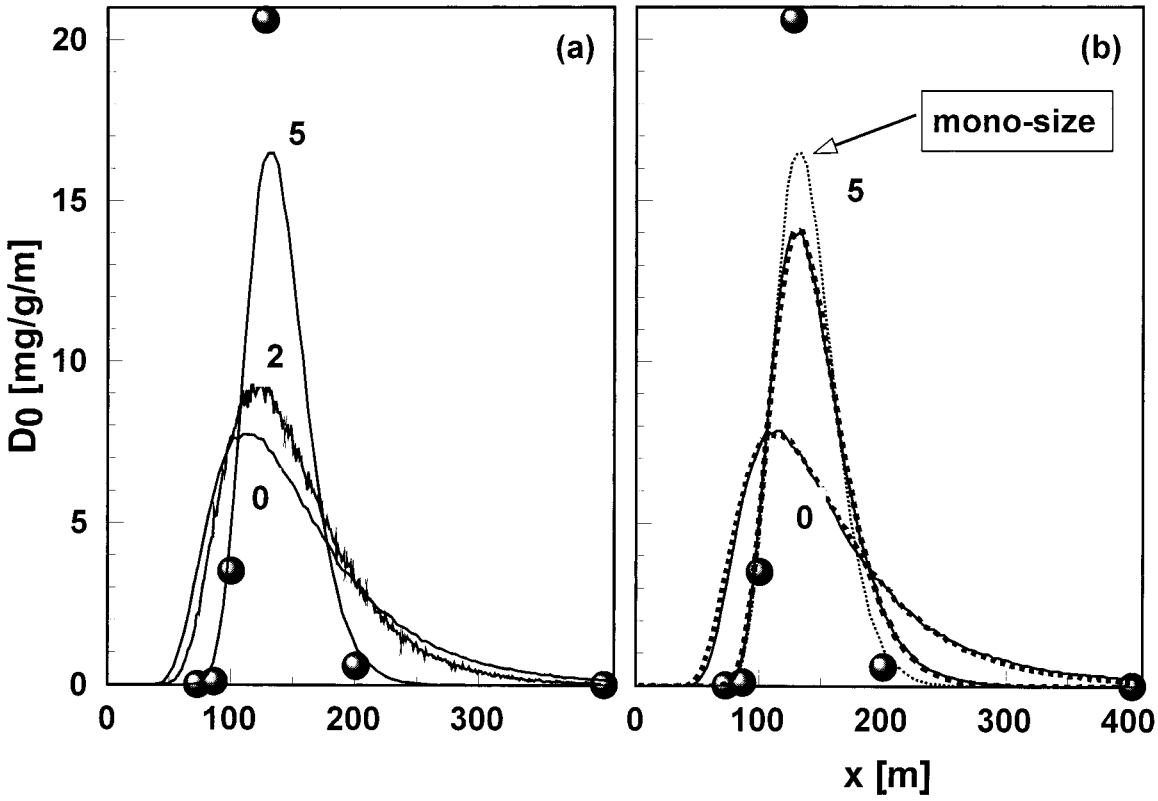

FIG. 5. Observations (●) and simulations of the alongwind profile of crosswind-integrated surface deposition rate, for the Suffield heavy particle dispersion trial A (stable stratification, $L = 30$ m; $R_{oA} = 1.0$). Particles ($w_g = 0.58$ m s^{-1}) released at $h = 15$ m. (a) Mono-size, one-dimensional simulations; Langevin for $\beta = (0, 5)$; and IP for $\beta = 2$. (b) Langevin simulations, with size-spectrum (except where noted), for $\beta = (0, 5)$. – – – one-dimensional, ——— two-dimensional.

of trial J are only weakly sensitive to the value specified for the timescale-reduction parameter β, not at all sensitive to specification of the (estimated) bead size spectrum, but there is a slightly more noticeable sensitivity to the alongwind fluctuation u' than was seen in other trials. This is not surprising, given that as source height (h) is reduced, the beads are injected into a wind with larger longitudinal turbulence intensity $\sigma_u(h)/\overline{u}(h)$.

Of all heavy particle dispersion trials here examined, simulations of trial A are least satisfactory (order 100% error). Trial A represents very stable stratification (in Hage's words, ''intense inversion at night in winter over frozen ground''). It is well to bear in mind that values of L assigned to these trials (Table 1) hinge on only a *single* measured vertical temperature difference, and that such differences can be troublesome to measure; simulations may perhaps not have properly represented the actual flow. Even if the trials *were* represented well by the scales given in Table 1, there is no doubt that micrometeorological theories, notably the Monin–Obukhov similarity theory according to which we anticipate definite interrelationships between the various flow properties (relationships we therefore embed in the trajectory models), are at the margin of their effectiveness in the very stable limit, for various well-understood reasons (including influence of surface slope; shallowness of the (putative) constant flux layer; possible radiative divergence; possible wave contribution to velocity fluctuations). Thus, we may regard the general capability of the Langevin model for particle trajectories as considerably better than is reflected by this worst (seen) case; perhaps the Langevin model, with β held constant ($\beta \approx 2$), more generally mimics ''reality'' to within about 20%.

4. Simulations of Elora heavy particle dispersion trials

In such contexts such as spore, pollen, or aerial spray transport, one's interest lies in trajectories near or within a tall canopy, a case lying outside the scope of the Suffield heavy particle dispersion trials. Wilson (1980) and Wilson et al. (1981; hereinafter WTK) reported concentration profiles of 40-μm diameter glass beads ($w_g = 0.12$ m s^{-2}; $\tau_p = 0.012$ s) at short distances from a continuous point source set above a corn crop. Source strength was known approximately, but a precise crosswind integration was not possible from the (only) three

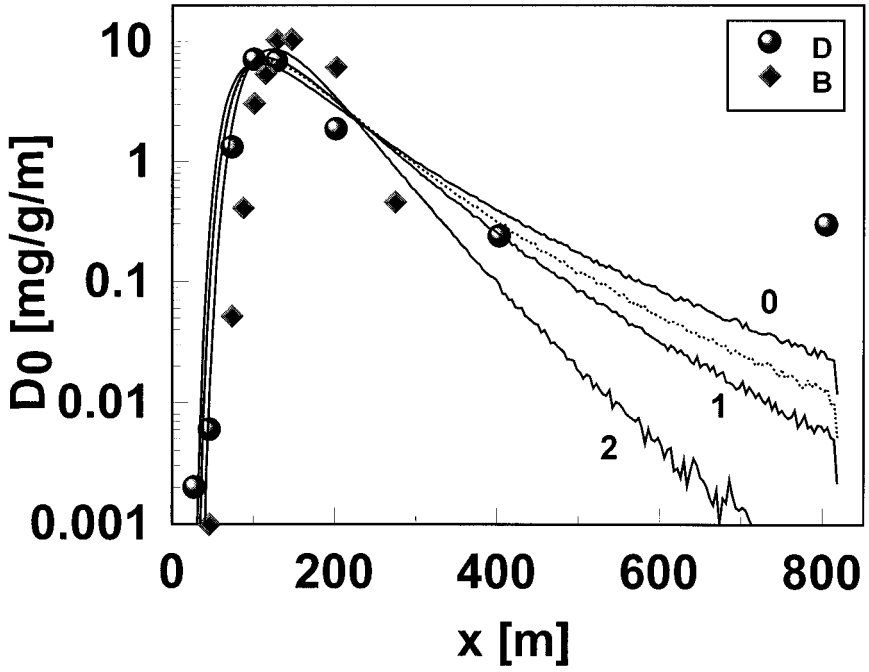

FIG. 6. Observations and simulations of the alongwind profile of crosswind-integrated surface deposition rate, for the Suffield heavy particle dispersion trials B, D (♦, ●), under weakly stable stratification ($L \approx 105$ m); recoveries $R_{oB} = 1.11$, $R_{oD} = 0.94$. Particles released at $h = 15$ m. Solid lines give Langevin simulations with monochromatic drop size ($w_g = 0.58$ m s^{-1}) for $\beta = (0, 1, 2)$. Dashed line gives Langevin simulation for spectrum of droplet sizes, with $\beta = 1$.

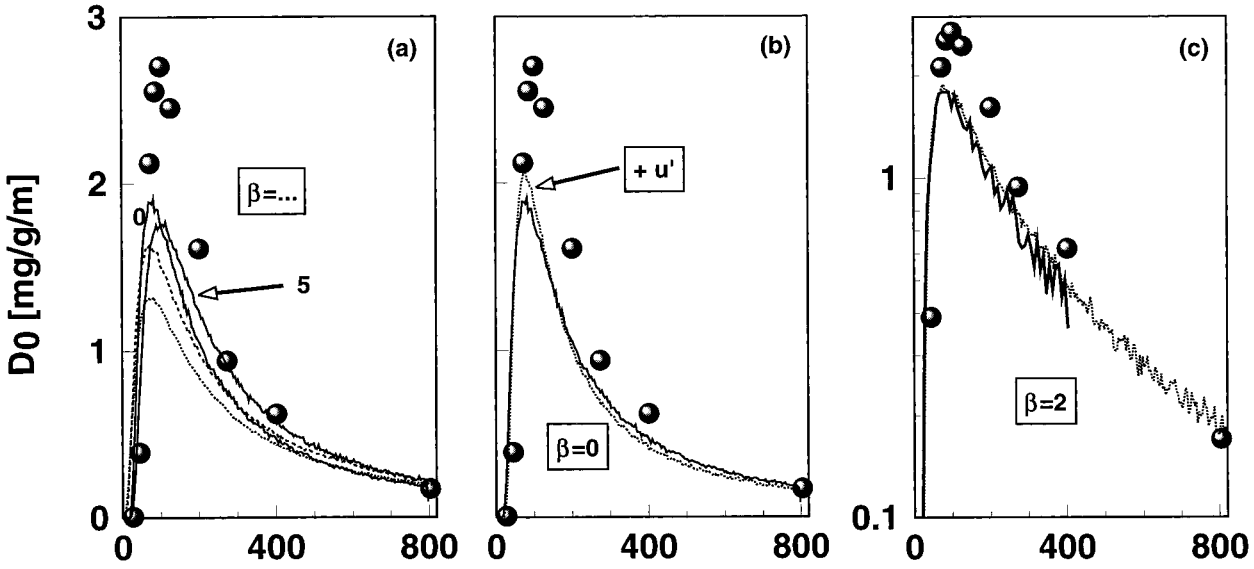

FIG. 7. Observations (●) and simulations of the alongwind profile of crosswind-integrated surface deposition rate, for the Suffield heavy particle dispersion trial J (unstable stratification, $L = -105$ m; recovery $R_{oJ} = 0.71$). Particles ($w_g = 0.14$ m s^{-1}) released at $h = 7.4$ m. (a) ····· RDM with $\Delta t = 0.1\Gamma_L(h)$, – – – RDM with $\Delta t = 0.1\Gamma_L(z)$, and ——— one-dimensional (no u') Langevin simulations with $\beta = (0, 5)$. (b) Influence of inclusion of u' (·····) vs otherwise (———), in Langevin simulation with $\beta = 0$. (c) Comparison of IP (———) and Langevin (– – –) treatments, with $\beta = 2$.

concentration masts. Cup anemometers provided the profile of mean wind speed $\overline{u}(z)$, and a sonic anemometer measured root-mean-square vertical velocity σ_w at a single height (z_{ref}) above the canopy.

a. 2D simulation of a ''no-canopy'' (large h/z_0) Elora trial

Figure 8 compares Langevin model simulations of the crosswind-integrated bead concentration profile [notation $\overline{c}(z)$ or $C(z)$] when the beads were released at height $h = 2.51$ m above a very sparse, short, immature crop ($h_c = 0.2$ m; trial of 2 July 1979 from WTK; $\sigma_w = 0.5$ m s^{-1}; $u_* = 0.4$ m s^{-1}). The point to be made is that model concentration profiles are sensitive not only to the timescale reduction (β), but also, and very vitally, to treatment of canopy absorption. Appreciable differences in near-ground concentration result from the alternative choices of perfect absorption at the roughness height z_0, or at crop height $h_c = 0.2$ m. Neither of these choices can be defended, in view of the small w_g/σ_w in these trials, which likely permitted ''reflection'' of some proportion of bead trajectories. But there is not sufficient information to attempt a rational treatment of absorption by this very low, sparse crop.

b. 3D simulation of ''full-canopy'' (small h/z_0) Elora trials

Wilson (1980) reported four experiments in which bead concentration profiles were observed at radius $x = 20$ m downstream from a source at $h = 2.35$ m, above a mature corn crop (fetch = 300 m; mean height $h_c = 2.1$ m; leaf area index LAI ≈ 2.8). Concentration profiles for the four trials were very similar, and experiment 1 (detailed on Table 2), which was performed during a strong and steady wind under an overcast sky (i.e., near-neutral stratification), can be taken as characteristic. Figure 9 gives the vertical profile of bead concentration c/Q (s m^{-3}), averaged across three masts placed so as to span the (visible) plume.

Throughout most of the depth of a tall canopy, it is believed that the Lagrangian timescale Γ_L is very large ($\Gamma_L \approx 0.3h_c/u_*$, Coppin et al. 1986). Therefore since the Langevin-class model has proved adequate to calculate particle trajectories well above the plants, there ought to be no fundamental difficulty in handling trajectories near or within the canopy. Flesch and Wilson (1992) found that an LS model for Gaussian inhomogeneous turbulence performed better (for tracer dispersion in a canopy) than models that attempted to account for the (actually) non-Gaussian Eulerian velocity statistics. Thus simulations here use Thomson's (1987) well-mixed multidimensional model for stationary, inhomogeneous Gaussian turbulence [Eq. (7), with an additional Langevin equation for a V' component uncorrelated with U' or W; and with a superposed gravitational settling velocity]. Appendix D details the parameterization of the wind and turbulence in the canopy. The time step was specified as $dt/\Gamma_p = 0.1$.

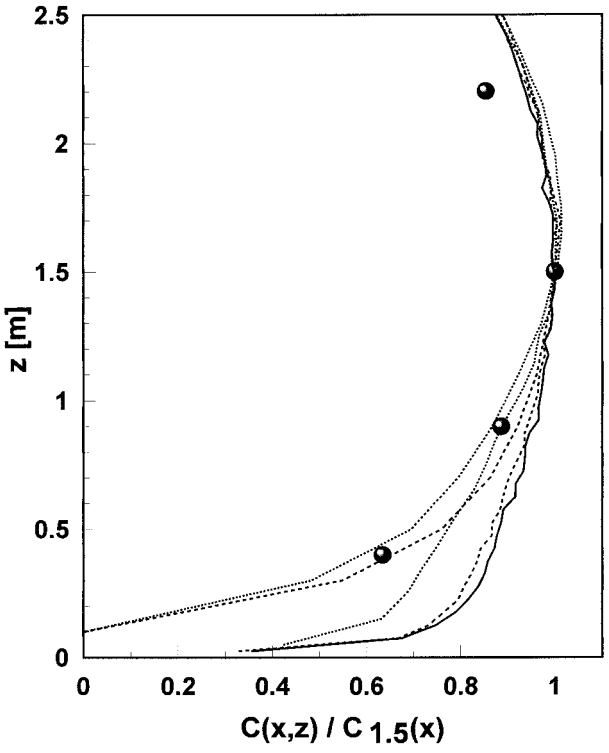

FIG. 8. Simulated and observed [●, Wilson et al. (1981) trial of 2 Jul 1979] vertical profiles of normalized concentration of glass beads ($w_g = 0.12$ m s^{-2}, $\tau_p = 0.012$ s) at distance $x = 20$ m downwind from a continuous source at height $h = 2.51$ m above sparse, immature corn (canopy height $h_c = 0.2$ m). Simulations use the Langevin-class model, and indicate sensitivity to timescale reduction (β) and height of ''surface'' absorption $z_{ab} = (z_0$ or $h_c)$. Solid line duplicates simulation by WTK, $\beta = 0$, $z_{ab} = z_0$; dashed lines, $\beta = 2$, with $z_{ab} = z_0$ or h_c; and dotted lines, $\beta = 5$, with $z_{ab} = z_0$ or h_c.

Upper leaves of plants near the source were literally ''dusted'' with beads, but deposition was not measured. In simulations, probability of deposition onto the vegetation during time step Δt can be treated as the product of the probability P_i that during that segment of its path the particle should intercept canopy elements, and the probability P_c of its resultant capture. Probability of capture P_c must parameterize unresolved details of the wind and particle trajectories near the plant parts, but interception probability is proportional to the step length (resolved velocity), and to the plant area density. As a particle trajectory model resolves instantaneous particle velocities, the probability of particle deposition P_D over any timestep Δt can be expressed as[5]

[5] Whereas canopy dispersion models based on the advection–diffusion equation (e.g., Legg and Powell 1979) necessarily parameterize deposition in terms of the (knowable) mean horizontal and vertical velocities, $\overline{s}(z)$ and w_g.

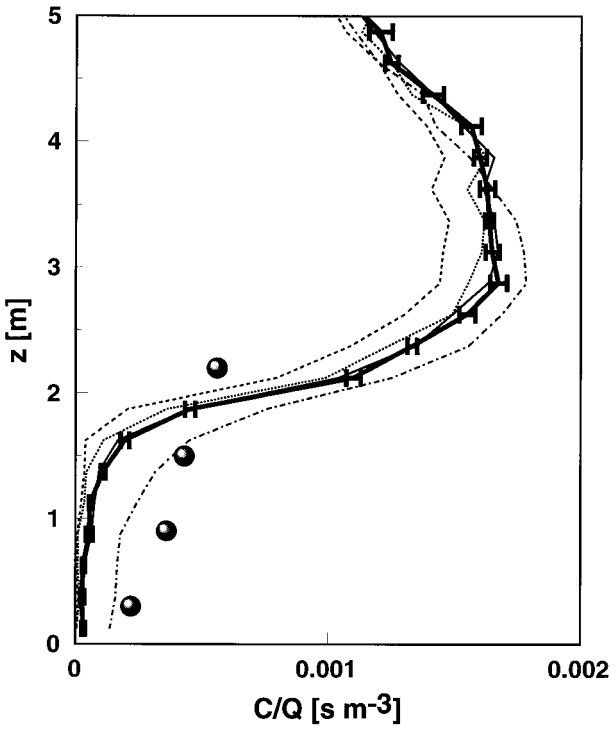

FIG. 9. Simulations of plume centerline concentration c/Q of glass beads, in and above a corn crop (canopy height $h_c = 2.1$ m), at distance $x = 20$ m downstream from a point source at height $h = 2.35$ m (experiment 1, Wilson 1980). Variation in observed concentration at $z = 2.2$ m, across the 3 masts, was about $\pm 25\%$. For all simulations, $A_x^2 = A_z^2 = \frac{1}{2}$, $P_{cz\uparrow} = 0$. Heavy solid: $\beta = 2$, $P_{cx} = 0.5$, $P_{cz\downarrow} = 0.5$ (bars give standard error). Light solid: $\beta = 0$, $P_{cx} = 0.5$, $P_{cz\downarrow} = 0.5$. Long-dash: $\beta = 0$, $P_{cx} = 0.95$, $P_{cz\downarrow} = 0.5$. Short-dash: $\beta = 0$, $P_{cx} = 0.5$, $P_{cz\downarrow} = 1$. Dot-dash: $\beta = 0$, $P_{cx} = 0.3$, $P_{cz\downarrow} = 0.3$.

$$P_D = [\sqrt{U_p^2 + V_p^2}P_{cx}A_z(z) + |W_p|P_{cz}A_x(z)]A(z)\Delta t(z), \quad (14)$$

where $A(z)$ is the leaf area density, A_x and A_z are the projection-factors thereof onto horizontal and vertical planes, and P_{cx}, P_{cz} are capture probabilities for the horizontal and vertical directions. The value P_{cz} can logically be partitioned according to the sign of the vertical velocity as

$$P_{cz} = \begin{cases} P_{cz\Uparrow}, & W_p > 0 \\ P_{cz\Downarrow}, & W_p < 0. \end{cases} \quad (15)$$

Equations (14) and (15) are physically plausible, but involve many parameters that are difficult to estimate, as well as the profile of leaf area density, which was not measured. The simulated plume-centerline concentration profile was highly sensitive to the leaf area density profile,[6] and to the alternative specifications of W_p or (more familiarly, but less justifiably) w_g as the velocity controlling probability of (vertical) interception of plant surfaces. As indicated by Fig. 9, over the range tested, simulations are more sensitive to variations in the several (unknown) deposition parameters than to the timescale reduction parameter β; that is, uncertainty in regard to the trajectory model itself is eclipsed by uncertainties w.r.t. deposition. And irrespective of the values of the deposition parameters, calculations produced a strong concentration gradient $\partial\overline{c}/\partial z$ near the top of the canopy, in contrast to the observed profile, which does not (in any obvious way) reflect the fact that the uppermost observation level ($z = 2.2$ m), lying slightly below the mean canopy height (which was estimated that day by sampling 35 plants distributed along the bead plume; mean $h_c = 2.1$ m, standard deviation $\sigma_{hc} = 0.08$ m), was in a region of strong vertical gradient in deposition probability (large $\partial\overline{s}/\partial z$ and $\partial A/\partial z$). Perhaps this is an indication that the profile of leaf area density assumed is unrealistic.

5. Conclusions

The ''Langevin class'' heavy particle trajectory model used in many of the preceding simulations is not new, having been used by Wilson et al. (1981) to simulate bead dispersion experiments, and more recently by Wang et al. (1995) in the treatment of aerial sprays. Current findings confirm the usefulness of this simple scheme for the calculation of an ensemble of heavy particle trajectories released from ''high'' sources (large h/z_0) in the unperturbed atmospheric surface layer. The RDM is clearly inferior, while the inertial particle model is superfluous.

Some qualification of that last statement is warranted. Very near ground, where τ_p/Γ_L is *not* small, and particle inertia reduces the particle velocity variance, trajectories *ought* to be calculated using an inertial particle model, for example, because a turbophoretic flux (Caporaloni et al. 1975; Reeks 1983; Brooke et al. 1994) of particles down the near-ground gradient in particle velocity variance cannot occur in the Langevin-class model. But there is an inevitable superficiality in the treatment of wind and dispersion very near ground, within what Wilson and Flesch (1993) have termed the ''Unresolved Basal Layer'' (UBL). Over the range of (u_*, L, z_0, h, τ_p, w_g) space covered in these atmospheric experiments, the observations here considered do not permit to distinguish any disadvantage of the Langevin model relative to the inertial particle model, for calculations of *practical* relevance. Evidently statistics of the particle concentration- and deposit-clouds will most often be calculated by a Langevin model to within an accuracy of about 20%, except near the outer fringes of the pattern.

Is this ''good enough''? It is probably fair to say that micrometeorological techniques and theories are rarely, in practice, more accurate than, very roughly, 20%—

[6] Results shown use that of Wilson (1988) for a corn canopy of the same LAI at the same site.

TABLE 2. Mean wind speed (* denotes intermittent stalling) and bead concentration profiles (masts A, B, C spanned plume centerline) from Elora glass bead dispersion experiment of 15 Aug 1979. Duration of release 1145–1545 EST (T = 240 min); sky condition, 8/10–10/10 cumulus of little vertical development; standard deviation of vertical velocity at $z = z_{ref}$ = 2.5 m (sonic anemometer) σ_w^{ref} = 0.86 m s^{-1}; from eight consecutive 30-min mean wind speeds at z = 4.23 m, mean wind speed $\bar{s}(4.23)$ = 5.02 m s^{-1} with $\sigma_{\bar{s}}/\bar{s}$ = 0.07 (std dev of 30-min means divided by 240-min mean). Bead source strength $Q \approx 1.5 \times 10^6$ (beads per second).

z (m)	U (m s^{-1})	C(A) (m^{-3})	C(B)	C(C)	C_avg (m^{-3})	C_avg/Q (s m^{-3})	C_norm
4.23	5.02						
3							
2.87	3.97						
2.2		1080	630	810	840	0.00056	1.3
1.88	2.21						
1.5		870	530	540	650	0.00043	1
1.08	0.82*						
0.9		640	430	550	540	0.00036	0.84
0.54	0.84*						
0.3		320	320	350	330	0.00022	0.51

for example, the common failure of surface heat- and latent-heat fluxes measured by eddy correlation to account for available radiant energy (Blanken et al. 1998), or disparities between surface-air trace-gas fluxes measured by alternative techniques.[7] That broad limit to attainable accuracy is in large measure due to inevitable discrepancies between the ''real world'' circumstances of measurements and idealizations inherent to the flow/dispersion models and the measurement techniques, the most important being idealizations of symmetry (e.g., horizontal homogeneity and/or stationarity), and of the adequacy of one's sampling of the (stochastic) system. An ''attainable accuracy'' for the random-flight heavy particle models of (only) about 20% is therefore not too far out of line with what is practically achievable.

Acknowledgments. I thank Drs. T. K. Flesch and P. A. Taylor for their helpful comments on this paper. Financial support of the Natural Sciences and Engineering Research Council of Canada (NSERC) is acknowledged.

APPENDIX A

Particle (vs Fluid-Lagrangian) Velocity Autocorrelation Timescale

Taking two key particle parameters τ_p and w_g, which suffice to characterize the simplest types of particles, and two fluid turbulence parameters (σ, Γ_L), we have two nondimensional ratios (τ_p/Γ_L, w_g/σ), and if we consider τ_p/Γ_L to be small enough, these two notional limiting cases:

1) If $\tau_p/\Gamma_L \ll 1$ and $w_g/\sigma \ll 1$, the driving velocity correlation reduces to the fluid Lagrangian correlation, and the timescale Γ_p is simply $\Gamma_p = T_L$.
2) If $\tau_p/\Gamma_L \ll 1$ but $w_g/\sigma \gg 1$, the particle is essentially always falling through the fluid at its terminal velocity, that is, it takes a ballistic trajectory through the eddy. If the time step is Δt ($\ll T_L$) then the particle traverses distance $w_g\Delta t$ through the eddy in each time step, during which time the eddy velocity is essentially unchanged. Then we can estimate a temporal correlation timescale along the particle trajectory as L_E/w_g where L_E is the Eulerian length scale.

Following Csanady (1963), Sawford and Guest assumed the correlation timescale Γ_p along a heavy particle trajectory to be an interpolation in w_g/σ between these limiting cases,

$$\Gamma_p = \frac{T_L}{\sqrt{1 + \left(\frac{\beta w_g}{\sigma}\right)^2}}. \qquad \text{(A1)}$$

Here $\beta = \sigma T_L/L_E$ is an empirical dimensionless constant that in principle differs, by a factor of 2, for velocity components parallel and perpendicular to the external force.[8] Sawford and Guest found that for dispersion *lateral* to the external force, their trajectory model was in reasonably good agreement with the laboratory experiments of Snyder and Lumley (1971) if they set $\beta = 3$ (but note the variance in terminology here relative to their paper).

[7] One may easily cite exceptions. This figure is meant to apply, not to instrumental limitations (e.g., achievable accuracy in measuring a mean vertical temperature difference), but to areally representative micrometeorological process rates, such as evaporation from a large lake or field, or wind reduction by a long shelterbelt, etc.

[8] Because the external force (**g**) in the atmospheric experiments to be considered is *parallel* to the most important fluctuation velocity (W_p), when Γ_p is reduced according to Eq. (A1), the constant β has (in principle) a value of *one-half* that found by Sawford and Guest to be optimal for dispersion lateral to the external force; that is, in the current case $\beta = 3/2$ is consistent with Sawford and Guest. However, it is a very long stretch between the ideal turbulence envisaged by those authors and the atmospheric case, and there is no reason to treat β as other than (again) a flexible parameter of order unity.

APPENDIX B

Surface-Layer Scales and Parameterization of Velocity Statistics for the Suffield Experiments

Outside (any) roughness sublayer, the state of the horizontally homogeneous atmospheric surface layer is characterized by scales u_*, L, z_0, and δ (friction velocity; Monin–Obukhov length; roughness length; and boundary layer depth, here unknown, but not critical). Best fit surface layer scales u_*, L were determined for the 12 Suffield trials that Walker labeled A–L, using the ($N_u \leq 5$) measured mean wind speed differences ($\Delta\overline{u}^m$), and the ($N_T = 1$) measured mean vertical temperature difference (ΔT^m). This was accomplished by adopting the standard Monin–Obukhov similarity theory for the vertical profiles of mean wind speed ($\overline{u}$) and temperature (T)

$$\frac{k_v z}{u_*}\frac{\partial \overline{u}}{\partial z} = \varphi_m\left(\frac{z}{L}\right) \quad \text{and} \tag{B1a}$$

$$\frac{k_v z}{T_*}\frac{\partial \overline{T}}{\partial z} = \varphi_h\left(\frac{z}{L}\right) \tag{B1b}$$

with von Kármán's constant $k_v = 0.4$. Following Dyer and Bradley (1982), it was assumed that for unstable stratification the universal functions are

$$\varphi_m = \left(1 - 28\frac{z}{L}\right)^{-1/4}, \quad \varphi_h = \left(1 - 14\frac{z}{L}\right)^{-1/2}, \tag{B1c}$$

while for stable stratification

$$\varphi_m = \varphi_h = 1 + 5\frac{z}{L}. \tag{B1d}$$

Integration between any pair of levels permits to deduce a *theoretical* temperature difference ΔT^{th} and wind speed difference $\Delta\overline{u}^{\text{th}}$, for any trial value of u^*, T^*. For each such "trial state," a residual was defined as $R = (1/\delta u^2)\ \Sigma\ (\Delta\overline{u}^m - \Delta\overline{u}^{\text{th}})^2 + (1/\delta T^2)(\Delta T^m - \Delta T^{\text{th}})^2$, where the normalizing factors δu ($=0.05$ m s^{-1}) and δT ($=0.2$ K) give relative weight to wind speed and temperature errors, and were given these values rather arbitrarily as representing reasonably realistic figures for instrument accuracy. Table (1) gives details of the trials, and the values of u_*, L corresponding to the smallest profile-fit residual R. The values given for roughness length z_0 were obtained by least squares fit to the observed wind profile, after having first optimized u_*, L. These fitted MO profiles generally agree very closely with the reported profiles, and parameters [e.g., z_0, and the wind speed at source height $\overline{u}(h)$] derived from them by Hage.

For the particle trajectory simulations of section 3, the stability-corrected mean wind profile $\overline{u} = \overline{u}(z)$ was specified according to Monin–Obukhov similarity (as above). The standard deviation for vertical velocity was specified as (Kaimal and Finngan 1994, p. 16)

$$\frac{\sigma_w}{u_*} = \begin{cases} 1.25\left(1 - 3\dfrac{z}{L}\right)^{1/3} & L < 0 \\ 1.25\left(1 + 0.2\dfrac{z}{L}\right) & L > 0, \end{cases} \tag{B1e}$$

while, in the few cases where U' was included, the oversimplification $\sigma_u = 2u_*$ was applied.

The Lagrangian timescale, or rather the equivalent compound variable $C_0\varepsilon$, was parameterized as

$$\frac{2\sigma_w^2}{C_0\varepsilon} = T_L(z) = \begin{cases} \dfrac{z}{2\sigma_w}\left(1 - 6\dfrac{z}{L}\right)^{1/4}, & L < 0 \\ \dfrac{z}{2\sigma_w}\left(1 + 5\dfrac{z}{L}\right)^{-1}, & L > 0. \end{cases} \tag{B1f}$$

This was found by Wilson et al. (1981) to result in good LS simulations of the Project Prairie Grass observations of tracer dispersion, across a wide range in stratification [Wilson and Shum (1992) reexamined and confirmed that finding after introduction of the wmc had clarified LS model construction].

In the neutral limit, the above choices reduce to $\sigma_w/u_* = b = 1.25$, and $T_L = \alpha z/\sigma_w$ with coefficient $\alpha = \frac{1}{2}$. Assuming for the neutral ASL that $\varepsilon = u_*^3/(k_v z)$ with $k_v = 0.4$, then α is related to the universal Kolmogorov coefficient C_0 according to

$$\alpha \equiv \frac{2\sigma_w^3}{C_0\varepsilon z} = 2\left(\frac{\sigma_w}{u_*}\right)^3\frac{k_v}{C_0} = 2b^3\frac{k_v}{C_0}, \tag{B1g}$$

and the current choices are consistent with $C_0 = 3.1$.

TABLE C1. Definition of five representative particle sizes to characterize the size-distributions of the beads released in the Suffield experiments, and the associated particle-release proportions (f_i) and settling velocities (w_{gi}). The five particle-size bins exclude about 5%–10% of the mass actually released as very small or very large particles, the purpose here being simply to assess the sensitivity of simulations to there being a size spectrum of some width. Data are given for beads with mass mean diameters $d_0 = (107, 49)$ μm, for which mass mean terminal velocities given by Walker (1965) were $w_{g0} = (0.58, 0.14)$ m s^{-1}.

Bin (i)	Range (μm)	d (i)	$f(i)$, %	$wg(i)$, m s^{-1}
1	95–100	97.5	13	0.48
2	100–105	102.5	33	0.53
3	105–110	107.5	30	0.58
4	110–115	112.5	18	0.64
5	115–120	117.5	6	0.69
1	42–45	43.5	19	0.11
2	45–48	46.5	28	0.13
3	48–51	49.5	26	0.14
4	51–54	52.5	18	0.16
5	54–57	55.5	9	0.18

Here, C_0 has been treated as an optimizable coefficient by most authors of LS models, in a manner equivalent to the optimization by Wilson et al. of α. Du et al. (1995) attempted to once and for all ''fix'' the value of C_0 by application of LS models to tracer dispersion experiments from the laboratory, but different authors continue to report as optimal, values quite far from the 3 ± 0.5 recommended by that study. Some of the authors (e.g., Edson and Fairall 1994) who continue to calibrate ASL trajectory models explicitly in terms of α (rather than C_0), prefer that value ($\alpha \approx 0.3$) that derives from equating the nominal far field mass diffusivity $\sigma_w^2 T_L$ to the neutral-limit eddy viscosity $K = k_v u_* z$, an identification that is supported by some of the surface-layer flux-gradient experiments on heat, momentum, and vapour transport, for example, Dyer and Bradley (1982), but leads to poor agreement with the Project Prairie Grass observations (and others).

APPENDIX C

Accounting for the Particle Diameter Distribution in the Suffield Trials

Although the actual size distribution of the beads released was reported, deposit density D_0 was based on assigning to each particle deposited *the same mass* (Hage 1961). Consequently reported D_0 is ''subject to errors due to the systematic decrease of mean particle diameter with distance from the source.'' Hage suggested (on the basis of measurements) that this error was probably negligible near the position of maximum deposit density, but might be up to 30%–40% (error in reported D_0) near the 5% and 95% cumulative mass limits of the deposit curve.

It is not possible retrospectively to determine the (true) mass-deposition density. However, it is perfectly possible to reproduce the error in D_0, however large or small that may be, in simulations; one need only subdivide the size spectrum into a number of classes (labeled ''i''), release the proper fraction $f_i = N_i/N_P$ of particles in each such class ($\Sigma_i N_i = N_P$ is the *total* number of trajectories calculated), apply the appropriate settling velocity w_{gi}, and *count* as if all particles had equal mass.

To assess the importance of the particle size distribution, the following procedure (which could be refined for higher fidelity) was used to determine the number fraction $f_i = N_i/N_P$ of particles to be released in each size class, in order to permit to more carefully represent the trials with the (nominally) 107 μm beads. A fourth-order polynomial,

$$CM = a_0 + a_1 d + a_2 d^2 + a_3 d^3 + a_4 d^4,$$

provided a good fit to the reported Cumulative Mass (CM) versus diameter (d) tabulations (Hage's Table 2; Walker's Table 1) over a diameter range encompassing more than 90% of the mass released; for the 107-μm and (in brackets) 49-μm beads, the coefficients were

$$a_0 = 73\,555.9 \qquad (6959.15)$$

$$a_1 = -2618.79 \qquad (-492.675)$$

$$a_2 = 34.664 \qquad (12.3928)$$

$$a_3 = -0.202\,23 \qquad (-0.128\,782)$$

$$a_4 = 0.000\,439\,3 \qquad (0.000\,455\,2).$$

Differentiating, one obtains a function $m = m(d)$ giving the mass fraction released per unit diameter range. Now of course, mass per particle varies as d^3, so the number of particles of any given diameter released per unit mass (of particles of that size) released, varies as d^{-3}. Then

$$n(d) = d^{-3} m(d) = a_1 d^{-3} + 2a_2 d^{-2} + 3a_3 d^{-1} + 4a_4,$$

is proportional to the number of particles released per unit diameter increment. Five particle-size bins were designated (Table C1), the number fraction of particles to be released for each bin was determined from $n(d)$, and each bin (i) was assigned a ''corrected'' settling velocity

$$w_{gi} = w_{g0} d_i^2 / d_0^2,$$

where w_{g0} is the figure given by Walker (1965) for the mass mean terminal velocity corresponding to mass mean diameter d_0.

APPENDIX D

Parameterization of Velocity Statistics in a Plant Canopy

Mean horizontal wind speed was parameterized as

$$\bar{s}(z) = \begin{cases} \bar{s}(h_c) \exp\left[\gamma\left(\dfrac{z}{h_c} - 1\right)\right], & z \le h_c \\ \bar{s}(h_c) + \dfrac{u_*}{k_v} \ln\left(\dfrac{z - d}{h_c - d}\right), & z > h_c, \end{cases} \qquad \text{(D1a)}$$

where it was assumed that $d/h_c = 0.67$. Speed at canopy height $\bar{s}(h_c)$ was inferred from the measurement $\bar{s}(4.23\ \text{m}) = 5.02\ \text{m s}^{-1}$, assuming friction velocity $u_* = \sigma_w^{\text{ref}}/1.25 = 0.69\ \text{m s}^{-1}$ (thus $\bar{s}(h_c) = 2.59\ \text{m s}^{-1}$, $\bar{s}(h_c)/u_* = 3.8$). By requiring the in-canopy exponential profile to fit the observed wind speed at $z = 1.88$ m, $\gamma = 1.5$.

Velocity standard deviations and shear stress were parameterized as

$$\sigma_{u,w}(z) = \begin{cases} \sigma_{u,w}^{\text{ref}}\left(0.2 + 0.8\dfrac{z}{h_c}\right), & z \le h_c \\ \sigma_{u,w}^{\text{ref}}, & z > h_c \end{cases} \quad \text{(D1b)}$$

and

$$\frac{\tau(z)}{u_*^2} = \begin{cases} 1, & \dfrac{z}{h_c} \ge 0.9 \\ 0.3 + 4.67\left(\dfrac{z}{h_c} - 0.75\right), & 0.9 > \dfrac{z}{h_c} \ge 0.75 \\ 0.3\exp\left[7\left(\dfrac{z}{h_c} - 0.75\right)\right], & 0.75 > \dfrac{z}{h_c} \end{cases} \quad \text{(D1c)}$$

while the Lagrangian timescale was specified as

$$\Gamma_L = \max\left[0.3\frac{h_c}{u_*}, \frac{0.5(z-d)}{\sigma_w}\right]. \quad \text{(D1d)}$$

REFERENCES

Blanken, P. D., and Coauthors, 1998: Turbulent flux measurements above and below the overstory of a boreal aspen forest. *Bound.-Layer Meteor.,* **89,** 109–140.

Brooke, J. W., T. J. Hanratty, and J. B. McLaughlin, 1994: Free flight mixing and deposition of aerosols. *Phys. Fluids,* **6,** 3404–3415.

Caporaloni, M., F. Tampieri, F. Trombetti, and O. Vittori, 1975: Transfer of particles in nonisotropic air turbulence. *J. Atmos. Sci.,* **32,** 565–568.

Coppin, P. A., M. R. Raupach, and B. J. Legg, 1986: Experiments on scalar dispersion within a model plant canopy. Part II: An elevated plane source. *Bound.-Layer Meteor.,* **35,** 167–191.

Corrsin, S., 1974: Limitations of gradient transport models. *Advances in Geophysics,* Vol. 18A, Academic Press, 25–60.

Csanady, G. T., 1963: Turbulent diffusion of heavy particles in the atmosphere. *J. Atmos. Sci.,* **20,** 201–208.

Deardorff, J. W., 1978: Closure of second and third moment rate equations for diffusion in homogeneous turbulence. *Phys. Fluids,* **21,** 525–530.

Du, S., B. L. Sawford, J. D. Wilson, and D. J. Wilson, 1995: A determination of the Kolmogorov constant (C_0) for the Lagrangian velocity structure function, using a second-order Lagrangian stochastic model for decaying homogeneous, isotropic turbulence. *Phys. Fluids,* **7,** 3083–3090.

Dyer, A. J., and E. F. Bradley, 1982: An alternative analysis of flux-gradient relationships at the 1976 ITCE. *Bound.-Layer Meteor.,* **22,** 3–19.

Edson, J. B., and C. W. Fairall, 1994: Spray droplet modelling. Part 1: Lagrangian model simulation of the turbulent transport of evaporating droplets. *J. Geophys. Res.,* **99,** 25 295–25 311.

Flesch, T. K., and J. D. Wilson, 1992: A two-dimensional trajectory-simulation model for non-Gaussian, inhomogeneous turbulence within plant canopies. *Bound.-Layer Meteor.,* **61,** 349–374.

Graham, D. I., 1996: An improved eddy interaction model for numerical simulation of turbulent particle dispersion. *J. Fluids Eng. (Trans. ASME),* **118,** 819–823.

Hage, K. D., 1961: On the dispersion of large particles from a 15-m source in the atmosphere. *J. Meteor.,* **18,** 534–539.

Hashem, A., and C. S. Parkin, 1991: A simplified heavy particle random-walk model for the prediction of drift from agricultural sprays. *Atmos. Environ.,* **25A,** 1609–1614.

Kaimal, J. C., and J. J. Finnigan, 1994: *Atmospheric Boundary Layer Flows.* Oxford University Press, 289 pp.

Lakehal, D., P. G. Mestayer, J. B. Edson, S. Anquetin, and J.-F. Sini, 1995: Eulero-Lagrangian simulation of raindrop trajectories and impacts within the urban canopy. *Atmos. Environ.,* **29,** 3501–3517.

Legg, B. J., and F. A. Powell, 1979: Spore dispersal in a barley crop: A mathematical model. *Agric. Meteor.,* **20,** 47–67.

——, and M. R. Raupach, 1982: Markov chain simulations of particle dispersion in inhomogeneous flows: The mean drift velocity induced by a gradient in Eulerian mean velocity. *Bound.-Layer Meteor.,* **24,** 3–13.

Lightstone, M. F., and G. D. Raithby, 1998: A stochastic model of particle dispersion in a turbulent gaseous environment. *Combust. Flame,* **113,** 424–441.

MacInnes, J. M., and F. V. Bracco, 1992: Stochastic particle dispersion modeling and the tracer-particle limit. *Phys. Fluids,* **A4,** 2809–2824.

Pan, Y., and S. Banerjee, 1996: Numerical simulation of particle interactions with wall turbulence. *Phys. Fluids,* **8,** 2733–2755.

Pope, S. B., 1987: Consistency conditions for random-walk models of turbulent dispersion. *Phys. Fluids,* **30** (8), 2374–2379.

Reeks, M. W., 1977: On the dispersion of small particles in an isotropic turbulent field. *J. Fluid Mech.,* **83,** 529–546.

——, 1983: The transport of discrete particles in inhomogeneous turbulence. *J. Aerosol Sci.,* **14,** 729–739.

Sawford, B. L., and F. M. Guest, 1991: Lagrangian statistical simulation of the turbulent motion of heavy particles. *Bound.-Layer Meteor.,* **54,** 147–166.

Snyder, W. H., and J. L. Lumley, 1971: Some measurements of particle velocity autocorrelation functions in a turbulent flow. *J. Fluid Mech.,* **48,** 41–71.

Taylor, G. I., 1921: Diffusion by continuous movements. *Proc. London Math. Soc. Ser. 2,* **20,** 196–212.

Thomson, D. J., 1987: Criteria for the selection of stochastic models of particle trajectories in turbulent flows. *J. Fluid Mech.,* **180,** 529–556.

Walker, E. R., 1965: A particulate diffusion experiment. *J. Appl. Meteor.,* **4,** 614–621.

Walklate, P. J., 1987: A random-walk model for dispersion of heavy particles in turbulent flow. *Bound.-Layer Meteor.,* **39,** 175–190.

Wallace, D. J., J. J. C. Picot, and T. J. Chapman, 1995: A numerical model for forestry aerial spraying. *Agric. For. Meteor.,* **76,** 19–40.

Wang, Y., D. R. Miller, D. E. Anderson, and M. L. McManus, 1995: A Lagrangian stochastic model for aerial spray transport above an oak forest. *Agric. For. Meteor.,* **76,** 277–291.

Wilson, J. D., 1980: Turbulence measurements in a corn canopy and numerical simulation of particle trajectories in inhomogeneous turbulence. Ph.D. thesis, University of Guelph, Ontario, Canada.

——, 1988: A second-order closure model for flow through vegetation. *Bound.-Layer Meteor.,* **42,** 371–392.

——, 1989: Turbulent transport within the plant canopy. *Estimation of Areal Evapotranspiration,* T. A. Black et al., Eds., Int. Assoc. Hydrol. Sci. Publ. No. 177, 43–80.

——, and W. K. N. Shum, 1992: A re-examination of the integrated horizontal flux method for estimating volatilisation from circular plots. *Agric. For. Meteor.,* **57,** 281–295.

——, and T. K. Flesch, 1993: Flow boundaries in random-flight dispersion models: Enforcing the well-mixed condition. *J. Appl. Meteor.,* **32,** 1695–1707.

——, and B. L. Sawford, 1996: Lagrangian stochastic models for trajectories in the turbulent atmosphere. *Bound.-Layer Meteor.,* **78,** 191–210.

——, G. W. Thurtell, and G. E. Kidd, 1981: Numerical simulation of particle trajectories in inhomogeneous turbulence. III. Com-

parison of predictions with experimental data for the atmospheric surface-layer. *Bound.-Layer Meteor.,* **21,** 443–463.

——, E. P. Lozowski, and Y. Zhuang, 1988: Comments on a relationship between fluid and immersed-particle velocity fluctuations proposed by Walklate (1987). *Bound.-Layer Meteor.,* **43,** 93–98.

Yudine, M. I., 1959: Physical considerations on heavy particle diffusion. *Advances in Geophysics,* Vol. 6, Academic Press, 185–191.

Zhuang, Y., J. D. Wilson, and E. P. Lozowski, 1989: A trajectory-simulation model for heavy particle motion in turbulent flow. *J. Fluids Eng.,* **111,** 492–494.